Molecular-dynamics simulation on simple fluids: Departure from linearized hydrodynamic behavior of the dynamical structure factor

E. Enciso, N. G. Almarza, and V. del Prado
Departamento de Química Física I, Facultad de Ciencias Químicas, Universidad Complutense, 28040 Madrid, Spain

F. J. Bermejo
Instituto de Estructura de la Materia, Consejo Superior de Investigaciones Científicas, Serrano 123, 28006 Madrid, Spain

E. López Zapata and M. Ujaldón
Departamento de Arquitectura de Computadores, Universidad de Málaga, Plaza del Ejido s/n, 29013 Málaga, Spain
(Received 13 January 1994)

Large scale molecular-dynamics simulations have been carried out that are especially designed to explore the *intermediate* region of the (k, w) plane of simple fluids, in order to bridge the gap between the hydrodynamics and kinetic domains; the gap is, unfortunately, unreachable by present light and neutron scattering techniques. The density fluctuations were obtained in a wide range of wave vectors and frequencies, i.e., $0.007 < [k\ (\text{Å}^{-1})] < 0.4$ and $0.006 < [\omega\ (\text{THz})] < 100$, respectively, for a state point of ^{36}Ar close to solidification. The dynamical structure factors are analyzed under linearized hydrodynamics assumptions, and the departure from such behavior is studied through sound damping factor and the Landau-Placzec ratio for $k > 0.15$ Å^{-1}. The deviations of the thermal damping factors appear at $k > 0.05$ Å^{-1}, which can be described in terms of the Fixman correction with a correlation length of $\simeq 15$ Å. The dispersion curve of the sound peak gives an adiabatic sound velocity slightly smaller than the one obtained from thermodynamic derivatives, in qualitative agreement with light scattering data.

PACS number(s): 61.20.Ja, 61.20.Lc, 61.25.Bi

I. INTRODUCTION

The usual point of departure for the study of the microscopic dynamics of simple fluids [1] involves the definition of different spatial and time domains. Such an artificial division arises from assumptions built-in within current theoretical approaches, such as linearized hydrodynamics or kinetic theories, or from limitations of present day computer and scattering experiments. Each technique provides dynamical information in a narrow spatial or time window, covering a small area of the wave vector and frequency plane (k, w) of the system [1]. For long wavelength and low frequency the liquid ($k \ll k_c$ and $\omega \ll \omega_c$, where ω_c is the characteristic frequency of the order of the reciprocal collision time 10^{-13} sec and k_c is the characteristic wavelength of the order of the intermolecular distance 1 Å) can be adequately described by the equations of the linearized hydrodynamics [1]. In such a limit, the fluid behaves like an elastic continuum and the only input required for the calculation of the response functions is the thermophysical properties of the fluid at equilibrium, which are obtained from direct experiments or calculations. The Fourier spectra $S(k, \omega)$ of the intermediate scattering function, which gives the time correlation functions of density fluctuations, of liquid argon were obtained from light scattering (LS) techniques [2] showing the triplet Rayleigh-Brillouin peaks, and since $k < 0.002$ Å^{-1} the results were analyzed with linearized hydrodynamics. In the opposite limit, the region of wave vectors comparable with intermolecular separations, i.e., $k > 0.2$ Å^{-1} up to k_c, was studied for the same fluid by neutron scattering (NS) techniques [3,4] and by molecular-dynamics simulation (MD) through modeling the bulk liquid with a sample of the order of 10^3 particles enclosed in a cubic box with periodic boundary conditions (PBC's) [5–7]. Classical neutron scattering experiments in liquids such as Rb, Pb, or Ne evidenced the presence of the hydrodynamic modes for $k > 0.15$ Å^{-1}, showing different damping coefficients whose k dependence is not completely understood [1]. The neutron and computer results for liquid argon [3,5–7] generated substantial controversies since the absence of well defined excitations within the allowed kinematic range did not allow a model-free assessment regarding the presence of propagating density fluctuations at these length scales. However, the analysis of the experimental $S(k, \omega)$ data in terms of either kinetic theory [3] or generalized hydrodynamics (i.e., allowing a wave vector and frequency dependence for the transport coefficients) [6] evidenced the presence of an inelastic, albeit strongly damped, response. Recent developments in neutron Brillouin scattering have allowed the measurement of propagating density fluctuations in dense argon gas at high temperature and densities (0.25 and 0.65 times the critical values) [4] and enabled the exploration of the range of k values, where a description in terms of linearized hydrodynamics holds, evidence a smooth crossover from hydrodynamic to kinetic regimes. The aim of this paper is twofold: first, to explore the capability of MD techniques for studying density fluctuations of simple liquids according the spa-

tial range covered by the experimental window of LS and NS techniques, $0.005 < [k\ (\text{Å}^{-1})] < 0.15$ (it has to be assessed whether the relaxation time of density fluctuations at those low wave vectors is smaller than the duration of the simulation run), and second, to characterize the departure from the linearized hydrodynamics of the dynamics structure factor of simple liquids at high densities by using independent measurements of the necessary thermophysical properties.

II. SIMULATION METHODOLOGY

We have modeled the liquid by enclosing 5184 atoms in a rectangular parallelepiped of volume $824.88 \times 17.18 \times 17.18$ Å^3 with PBC's; in such a system we have collected the data to calculate the time correlation functions of density fluctuations. On the other hand, the thermodynamic and transport properties were obtained from small systems, 256 atoms enclosed in a cubic box of side length 22.9 Å with PBC's. The particles interact through a shifted Lennard-Jones (LJ) potential [8]

$$V(r) = \begin{cases} V_{\text{LJ}}(r) - V_{\text{LJ}}(r_c), & r < r_c \\ 0, & r > r_c, \end{cases}$$
$$V_{\text{LJ}}(r) = 4\epsilon\left[(\sigma/r)^{12} - (\sigma/r)^6\right]. \qquad (2.1)$$

The parameters σ, ϵ, and $\tau = (m\sigma^2/\epsilon)$ define the length, energy, and time units, respectively. The potential is cut off at $r_c = 2.5\sigma$, i.e., no particles interact beyond this range. We model the dynamics of real ^{36}Ar atoms by choosing the standard set $\sigma = 3.405$ Å, $\epsilon = 119.8k_B$, and $\tau = 2.047$ ps. The integration of the equations of motion was performed in the microcanonical ensemble (NVE ensemble) by using the leap-frog algorithm [8]. The thermodynamic derivatives such as heat capacities and isothermal compressibility were obtained from Monte Carlo (NPT ensemble) simulations [8] on the small sample. The initial configuration was obtained from melting a fcc structure, and during the equilibration part of the MD simulations the velocities of the atoms were scaled to achieve an average reduced temperature ($T^* = k_BT/\epsilon$) of 0.97. We have modeled a thermodynamic state of liquid ^{36}Ar close to the density of 0.0216 Å^{-3} and temperature of 120 K, which was measured in exhaustive experiments of neutron scattering [3], covering large wave vectors, i.e., $0.42 < [k\ (\text{Å}^{-1})] < 2.22$.

For saving computing time in the large sample we have divided the system in different cells along the larger side of the simulation box (x direction). The length of such cells in the x direction is chosen to be slightly greater than r_c. Therefore a particle in a cell will only interact with particles belonging to the same cell and particles belonging to the two next-neighbor cells. After the particle positions are updated the list of the particles in each cell must be updated to account for positional changes. During the integration of the equations of motion in the different MD runs we calculated the Fourier components of the microscopic number density, the six independent components of the stress tensor and the three components of the energy current, and kept them for later analysis. The length of the MD run in the large system was 2.5 ns and for the small one 20 runs of 1–2 ns were performed. The Monte Carlo (MC) NPT data were obtained from 10 independent runs of 8000 MC steps, i.e., each MC step move implies the random motion of each particle and one attempt of changing the volume.

III. RESULTS

The basic thermophysical quantities calculated from MD and MC runs are shown in Table I together with experimental data of argon for a close thermodynamic state [3]. The heat capacities at constant volume were obtained from fluctuations of the kinetic energy into the MD NVE runs and those corresponding to constant pressure as well as the isothermal compressibility from fluctuations of the enthalpy and the volume into the MC NPT runs. The isothermal compressibility shows good agreement with the extrapolated value of the structure factor $S(k)$ at the

TABLE I. Thermophysical properties of ^{36}Ar liquid and the LJ model at a thermodynamic state near solidification conditions. The results of actual argon were obtained from Table IV of van Well *et al.* [3] and for the model we obtain them from several independent MD NVE and MC NPT simulation runs.

Property	^{36}Ar	^{36}Ar	LJ (^{36}Ar)
Pressure p (MPa)	27	39	64(2)[a]
Temperature T (K)	120	120	116(4)
Density ρ (10^{-4}Å^{-3})	195	201	213
Specific heat at constant pressure c_p (10^{-23}J K^{-1})	6.90	6.70	6.70(2)
Specific heat ratio $\gamma = c_p/c_v$	2.17	2.04	1.90(2)
Structure factor $10^{-2}S(0)$	8.9	7.2	4.2(1)
Adiabatic sound velocity c_s (m s^{-1})	824(8)	886(9)	1110(20)
Shear viscosity η_s (10^{-5}kg m s^{-1})	15.4(5)	17.4(5)	22(2)
Longitudinal viscosity η_l (10^{-5}kg m s^{-1})	30(3)	31(3)	38(5)
Thermal diffusivity Γ_t (10^{-8} m^2 s^{-1})	8.2(2)	8.9(3)	7.7(7)
Sound damping factor Γ_s (10^{-8}m^2 s^{-1})	20(2)	21(2)	19(2)
Self-diffusion D_s (10^{-8} m^2 s^{-1})	0.49(1)	0.43(1)	0.26(2)

[a] The value of pressure is corrected corresponding to the full LJ potential.

lowest wave vectors. The transport coefficients were obtained from Kubo relations [1], from the analysis of the correlation functions of the stress tensor, and from energy current components; see Table I. The slow decays of the long tail and the low signal to noise ratio of those correlation functions at large times required several independent MD NVE runs for maintaining the statistical error within reasonable boundaries. Those properties were used to obtain the necessary parameters for a linearized hydrodynamic description of the density fluctuations.

We have obtained the intermediate scattering function $F_d(k,t)$ from the correlation function of the instantaneous microscopic density along the x direction, the largest side of the box,

$$\rho(k,t) = \sum_{j=1}^{N} \exp\left[-ik_x r_{xj}(t)\right], \tag{3.1}$$

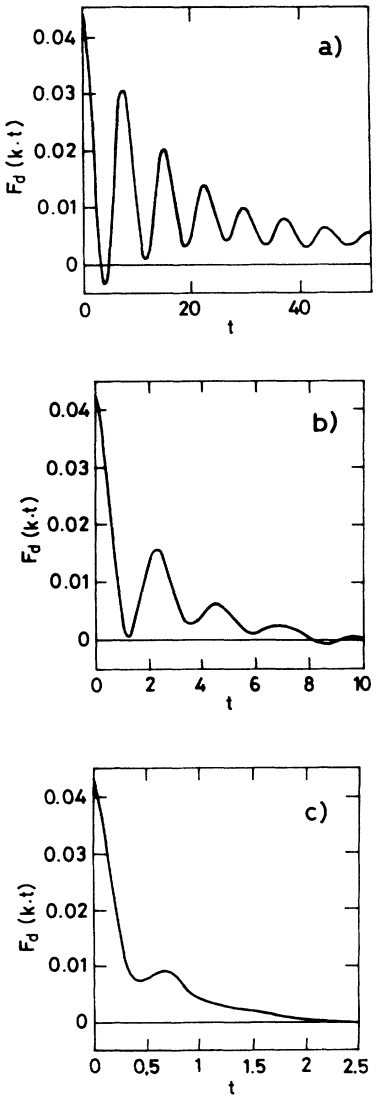

FIG. 1. Intermediate scattering function $F_d(k,t)$ at different wave vectors: (a) k=0.038, (b) k=0.122, and (c) k=0.366 in Å^{-1} units. The time is given in reduced units $t^* = t/\tau$.

$$F_d(k,t) = \frac{1}{N}\langle \rho(k,t)\,\rho(-k,0)\rangle, \tag{3.2}$$

where $r_{xj}(t)$ denotes the x coordinate of the particle j and the angular brackets denote an equilibrium ensemble average. The wave vectors k were defined along the x axis, as $k_n = 2\pi n/L_x$, and the integers n were chosen in the range 1–48, which covers the k domain of $0.007 < [k\ (\text{Å}^{-1})] < 0.366$, just the spatial range in between the light and neutron scattering experiments. In Fig. 1 the $F_d(k,t)$ are shown for several k values, evidencing the sinusoidal features of the sound mode at low k values, and when k increases, that mode becomes highly damped and indistinguishable from the thermal one. Those functions show an initially rapid decay followed by a distinctly slower relaxation with high noise to signal ratio which bounds the time window of this "numerical" experiment. The Fourier transform of $F_d(k,t)$ functions gives the coherent dynamical structure functions

$$S(k,\omega) = \frac{1}{2\pi}\int_{-\infty}^{+\infty} dt \exp(-i\omega t)\, F_d(k,t), \tag{3.3}$$

which is directly accessible in scattering experiments. The spectra obtained (see Fig. 2) fulfill the second moment condition $\langle w^2\rangle = (v_0 k)^2$ [1], where v_0 is the thermal velocity, but the evaluation of the fourth frequency moment w^4 was hindered by statistical noise in the data at high frequencies. We have fitted the spectra to the three peaks according the linearized hydrodynamic description, neglecting, according to the experimental uncertainty, the small non-Lorentzian contribution [1] and given by

$$S(k,\omega) = \frac{S(k)}{2\pi}\left[\left(\frac{\gamma-1}{\gamma}\right)\frac{2\Gamma_t k^2}{\omega^2 + (\Gamma_t k^2)^2} + \frac{1}{\gamma}\left(\frac{\Gamma_s k^2}{(\omega+\omega_s)^2 + (\Gamma_s k^2)^2} + \frac{\Gamma_s k^2}{(\omega-\omega_s)^2 + (\Gamma_s k^2)^2}\right)\right], \tag{3.4}$$

where $S(k)$ denotes the static structure factor, γ the ratio of heat capacities, $\Gamma_t = \lambda/(\rho c_p)$ the thermal diffusivity, λ the thermal conductivity, c_p the specific heat at constant pressure, $\omega_s = c_s k$, $\Gamma_s = [\eta_l + (\gamma-1)\Gamma_t]/2$ the dispersion relation of the sound mode, $c_s = \gamma k_B T/[mS(0)]$ the adiabatic speed of sound, $S(0)$ the zero-k limit of the $S(k)$ obtained from the isothermal compressibility $\kappa_T = S(0)/(\rho k_B T)$ the sound damping factor, $\eta_l = [\eta_v + (3/4)\eta_s]$ the longitudinal viscosity, η_v the bulk viscosity, and η_s the shear viscosity. The parameters of the fitted Lorentzians are shown together with the theoretical predictions [i.e., parameters of Eq. (3.4) obtained from the corresponding thermophysical properties shown in Table I] in Figs. 3–5. In Fig. 3 we display the sound frequency $\omega(k)$ as a function of k, which shows good agreement with theory from the adiabatic speed of sound of the LJ model in all range of wave vectors studied, with a slight deviation towards smaller values in good agree-

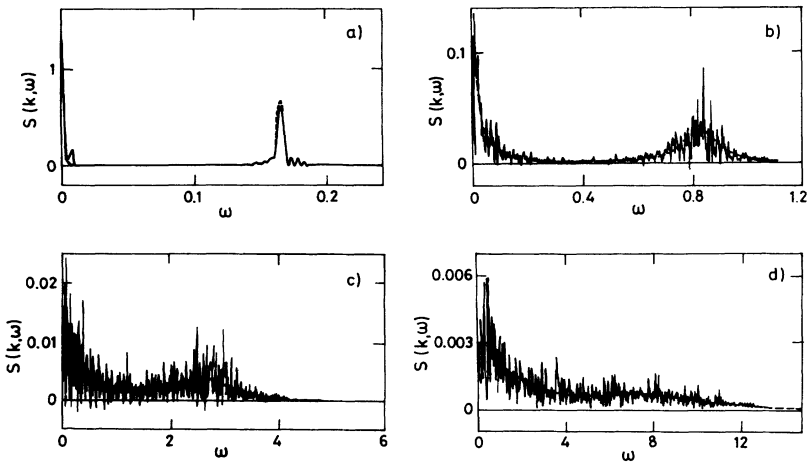

FIG. 2. Dynamic structure factor $S(k,\omega)$ [as obtained by a Fourier transform of the $F_d(k,t)$ functions of different wave vectors]: (a) k=0.0076, (b) k=0.038, (c) k=0.122, and (d) k=0.366 in Å^{-1} units. The dashed lines show the two fitted Lorentzians. The frequency is given in τ^{-1} units.

ment with earlier Brillouin scattering data of liquid argon [2]. The LJ model shows a slightly larger speed of sound, or smaller compressibility, than actual argon [3], which could explain the deviations observed in the dispersion curve from earlier MD simulations [7]. The k dependence of the width of the sound peak (see Fig. 4) agrees within the experimental error with theoretical predictions up to $k < 0.15$ Å^{-1}. In that range the behavior of the sound damping factor seems to tend toward a linear dependence on k, also observed in the width of real argon at $k < 1.2$ Å^{-1} [3]. Although the experimental resolution of the spectra is degraded at the lowest values or the wave vectors, a deviation of the linear behavior in the Rayleigh peak width divided by k for $k > 0.05$ Å^{-1} can be seen in Fig. 4. The damping of the thermal mode observed by experiment is larger than what can be expected from linearized hydrodynamics. Only in the vicinity of the critical points a similar behavior has been reported by LS techniques [9]. Such deviations can be accounted by the Fixman correction [10], which was originally derived by modifying the hydrodynamic equations by inclusion of the correlations of density between neighboring volume elements. The resulting linewidth divided by the wave vector thus gives

$$\Gamma k = \Gamma_t k \left[\left(1+\xi^2 k^2\right) / \left(1+\xi^2 k^2/\gamma\right) \right], \qquad (3.5)$$

where ξ is interpreted as a correlation length. The experimental values agree with Eq. (3.5) for wave vectors up to 0.15 Å^{-1} and by using a correlation length of 15 Å, close to the limit where we can observe the structure of the pair distribution function of the fluid. At large wave vectors we observe a crossover towards a linear behavior of the line width. The intensity ratio of the two peaks gives some information about the wave vector dependence of the heat capacities ratio; see Fig. 5. In the middle range of the region studied, $k < 0.2$ Å^{-1}, we observe good agreement with the theory; the deviations down to $k < 0.035$ Å^{-1} are within the experimental uncertainty of the dynamic structure factor given the low signal to noise ratio.

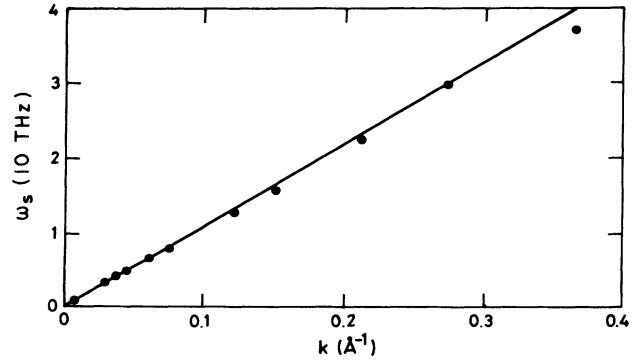

FIG. 3. Parameters of the linearized hydrodynamic model: peak position ω_s of the sound mode. Dots show the fitted parameters from $S(k,\omega)$ and the line the theoretical prediction.

IV. CONCLUSIONS

We have performed large scale MD and MC simulations on a LJ fluid modeling real liquid ^{36}Ar with the

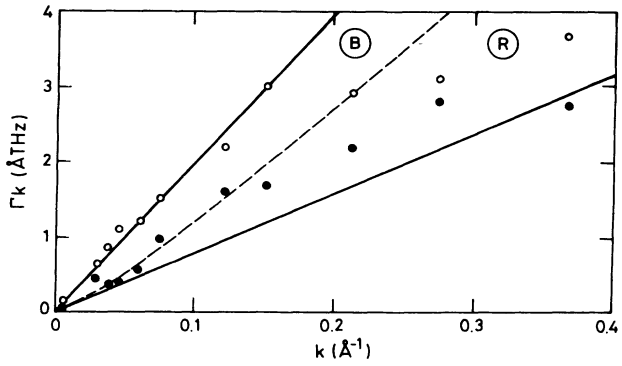

FIG. 4. Parameters of the linearized hydrodynamic model: widths of the Rayleigh-Brillouin peaks. Open circles and dots show the fitted parameters from $S(k,\omega)$ of the widths of the Brillouin and Rayleigh peaks, respectively. The continuous line shows the theoretical predictions and the dashed line the Fixman modification, given in Eq. (3.5).

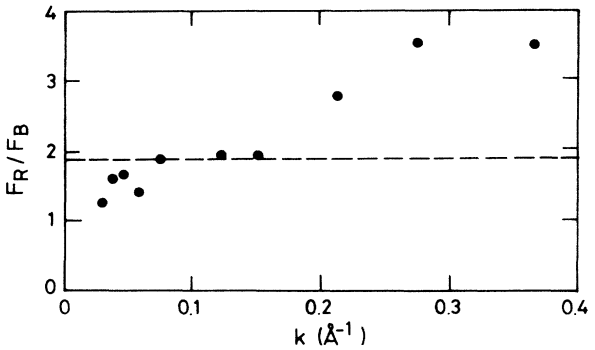

FIG. 5. Parameters of the linearized hydrodynamic model: ratio of the Rayleigh to Brillouin peak. Dots show the ratio from the fitted parameters and the dashed line the theoretical prediction.

goal of measuring the departure from the linearized hydrodynamics of the density fluctuations at wave vectors outside the window reachable by light and neutron scattering experiments. By using a large parallelepiped box, whose largest side is 825 Å, we have linked the spatial range covered by those scattering techniques, which by combining numerical and scattering results leads us to reach dynamical information of the fluid in a wide area of the (k, w) plane. The intermediate coherent functions obtained show the two contributions corresponding to thermal and sound modes. At large wave vectors the sound mode becomes indistinguishable from the thermal one. The linearized hydrodynamics using the thermophysical properties obtained can almost explain the wave vector dependence of the numerical spectra after fitting them to the two Lorentzian descriptions. We observe a small deviation of the dispersion relation of the sound mode with respect to the theoretical predictions. The width of the thermal is also larger than the values predicted by linearized hydrodynamics, although the deviations at $k < 0.15$ Å^{-1} can be accounted for by the Fixman correction, with a correlation length of 15 Å. A better quantitative description of those deviations leads us to increase the scale of the simulation, in order to reduce the statistical uncertainties, i.e., the signal to noise ratio of the intermediate scattering functions at low wave vectors. This is our next project, together with exploring the influence of the thermodynamic state of the fluid into density fluctuations in the intermediate region of the (k, w) plane.

ACKNOWLEDGMENTS

The authors acknowledge the financial support of DGXII/EEC Contracts Nos. CHRX-CT-93-0092/130 and ./1B0, and Grant No. PB92-0114-C04-02 of DGICYT, Spain. We thank J.L.F. Abascal, J.C. Gil, F. Ortega, and G. Tardajos for stimulating discussions.

[1] J.P. Boon and S. Yip, *Molecular Hydrodynamics* (McGraw-Hill, New York, 1980), and references therein; J. P. Hansen and I.R. MacDonald, *Physics of Simple Liquids* (Academic, New York, 1980), and references therein.

[2] P.A. Fleury and J.P. Boon, Phys. Rev. **186**, 244 (1969).

[3] A.A. van Well, P. Verkerk, L.A. de Graaf, J.-B. Suck, and J.R.D. Copley, Phys. Rev. A **31**, 3391 (1985); P. Verkerk and A.A. van Well, Physica **136B**, 1168 (1986).

[4] U. Bafile, P. Verkerk, F. Barocchi, L.A. de Graaf, J.-B. Suck, and H. Mutka, Phys. Rev. Lett. **65**, 2394 (1990).

[5] A. Rahman, Phys. Rev. Lett. **19**, 420 (1967).

[6] D. Levesque, L. Verlet, and J. Kürkijarvi, Phys. Rev. A **7**, 1690 (1973); D. Levesque and L. Verlet, Mol. Phys. **61**, 143 (1987); M. Schoen, R. Vogelsang, and C. Hoheisel, *ibid.* **57**, 445 (1986).

[7] I.M. de Schepper, J.C. van Rijs, A.A. van Well, P. Verkerk, L.A. de Graaf, and C. Bruin, Phys. Rev. A **29**, 1602 (1984); P. Verkerk, A.A. van Well, and I.M. de Schepper, J. Phys. C **20**, L979 (1987).

[8] M.P. Allen and D.J. Tildesley, *Computer Simulation of Liquids* (Oxford University Press, Oxford, 1989).

[9] H.G. Stanley, *Phase Transitions and Critical Phenomena* (Clarendon Press, Oxford, 1971).

[10] M. Fixman, J. Chem. Phys. **33**, 1363 (1960); W. Botch and M. Fixman, *ibid.* **42**, 199(1965); R.D. Mountain, Rev. Mod. Phys. **38**, 205 (1966); H.Z. Cummings and H.L. Swinney, J. Chem. Phys. **45**, 4438 (1966).